ASTRONOMY & ASTROPHYSICS
SUPPLEMENT SERIES

Astron. Astrophys. Suppl. Ser. **114,** 537-548 (1995)

A deep BVI photometric study of the open cluster NGC 2453*

D.C.V. Mallik, R. Sagar and A.K. Pati

Indian Institute of Astrophysics, Bangalore 560034, India

Received December 29, 1994; accepted June 21, 1995

Abstract. — CCD observations of the open cluster NGC 2453 have been carried out in B, V and I passbands. A total of 356 stars have been observed in a field of about $4' \times 6'$ of the sky centred on the cluster. Colour-magnitude diagrams in V, $B-V$ and V, $V-I$ have been generated down to $V = 20$ and for the first time, the unevolved part of the cluster main sequence has been observed. The mean true distance modulus derived from these diagrams is $13\overset{m}{.}85 \pm 0.2$ yielding a distance of 5.9 ± 0.2 kpc. A mean age of 25 Myr has been derived for the cluster by fitting isochrones. The distance of approximately 6 kpc puts the cluster much beyond the planetary nebula NGC 2452 whose largest estimated distance to date is about 3.5 kpc. The two are not physically associated.

Key words: open clusters: individual: NGC 2453 — stars: evolution — planetary nebulae: individual: NGC 2452 — HR diagram

1. Introduction

NGC 2453 ($\equiv$ C 0745 − 271 $\equiv$ OCL 670) located at $\alpha_{1950} = 07^h45\overset{m}{.}7$, $\delta_{1950} = -27°07'$, ($l = 243\overset{\circ}{.}33$, $b = -0\overset{\circ}{.}94$), is an open cluster of Trumpler class I3 m (Lyngå 1987) in Puppis which attracted our attention because of its angular proximity to the bright Type I planetary nebula NGC 2452 (PN G 243.3 − 01.0, PK 243 − 1° 1). The planetary nebula is located approximately $8'.5$ southwest of the cluster. Gathier (1984) included the cluster in his programme on photometry of stars in the region of NGC 2452 to determine an improved reddening - distance relation for the nebula. The cluster was previously studied by Seggewiss (1971) and Moffat & Fitzgerald (1974, hereafter MF). Seggewiss determined a distance of 1490 pc based on the photoelectric photometry of only six stars brighter than $V = 14^m$. Moffat observed a larger sample of twenty one stars photoelectrically in U, B and V. These were supplemented by photographic observations of another seventy two stars (MF) up to a limiting magnitude $V = 15.5$. Reddening parameters were derived from a colour - colour plot, the mean $E(B-V)$ based on photoelectric measurements of 7 B stars being $0\overset{m}{.}47 \pm 0.04$. Distance was obtained by fitting the main sequence on both V, $B-V$ and V, $U-B$ diagrams yielding the result, $V_0 - M_v = 12\overset{m}{.}33 \pm 0.2$ which corresponds to a distance $D = 2.9 \pm 0.2$ kpc. The distance was thus twice the value found by Seggewiss (1971). Since there was considerable spread in the data on the colour-magnitude diagrams for the cluster and only the upper main sequence was discernible, the estimated distance was not deemed very reliable and Gathier (1984) redetermined the reddening and the distance modulus by using Walraven photometry on five nearly certain members of the cluster. While the colour excess, he found, was almost the same as before ($E(B-V) = 0\overset{m}{.}49 \pm 0\overset{m}{.}01$), the new distance modulus was considerably different, $V_0 - M_v = 13\overset{m}{.}48 \pm 0.26$ corresponding to $D = 5.0 \pm 0.6$ kpc. Gathier also obtained a distance to the nebula NGC 2452 from the reddening - distance diagram where the point corresponding to the distance and reddening of NGC 2453 was treated as the most accurate one and this turned out to be 3.47 ± 0.5 kpc. While the distances to NGC 2452 and 2453 were thus discrepant, the following two quite independent pieces of data pointed to a possible physical association of the cluster with the nebula:

- 1) The radial velocity of NGC 2452 was measured by Campbell & Moore (1918) to be + 68 km s^{-1} and the radial velocity of an evolved blue giant in the cluster field was estimated as 67 ± 14 km s^{-1} (MF).
- 2) The $E(B-V)$ colour excesses of the cluster and the nebula were found to be very similar being $0\overset{m}{.}47$ and $0\overset{m}{.}43$ respectively.

To settle unambiguously the question of the distance to the cluster and that of its physical connection to NGC 2452, we decided to undertake a deep CCD photometric study of the cluster. Observations were carried out in B, V and I passbands on seven nights between 1989 March and 1992 March using a CCD photometer at the Cassegrain focus of the 1.02 m Zeiss telescope at Vainu Bappu

*Table 3 only available in electronic form at CDS via ftp 130.79.128.5

Observatory, Kavalur, India. These were supplemented by observations in B and V in 1994 February using a CCD photometer at the prime focus of the 2.34 m Vainu Bappu Telescope at the same observatory. We reached down to $V = 20$ with good signal -to - noise ratio and were able to locate the unevolved part of the cluster main sequence. Since we did not observe in U, we could not independently estimate the reddening of the cluster. For $E(B-V)$ we use the value of $0\overset{m}{.}47$. From the colour magnitude arrays in $V, B-V$ and $V, V-I$ with appropriate main sequence fitting procedures we obtain a mean true distance modulus, $V_0 - M_v = 13\overset{m}{.}85 \pm 0\overset{m}{.}2$ and hence a distance of 5.9 $\pm$ 0.2 kpc for the cluster.

A preliminary analysis of our data in V and I was presented in the IAU Symposium 155: Planetary Nebulae (Mallik et al. 1993). The present work incorporating new data in B with the larger telescope supersedes the earlier results. We rule out any possible association of the cluster with the nebula NGC 2452, the latter being almost certainly a foreground object as its distance has been variously estimated to lie in the range 1400 to 3500 pc (Gathier 1984).

In Sect. 2 we discuss in detail the observations and the data reduction procedures. This is followed in Sect. 3 by a presentation of the results. We conclude with a critical discussion of the results in Sect. 4.

1.1. *Observations*

The deep colour-magnitude diagrams of the cluster have been generated from the observations in B, V and I passbands taken at the $f/13$ Cassegrain focus of the 102 cm Zeiss telescope and the $f/3.23$ prime focus of the 234 cm Vainu Bappu Telescope located at the Vainu Bappu Observatory (VBO) in Kavalur, India. The log of the observing runs is given in Table 1. The 234 cm telescope was used mainly to obtain deep CCD frames in the B filter with good signal-to-noise ratio. There was no need to observe with the I filter at this telescope since observations with the 102 cm telescope were found adequate.

At the 102 cm telescope we used a Thomson - CSF TH 7882 CCD chip with the format 384 $\times$ 576 pixels. The pixel size of 23 μm square corresponds to 0.36 arcsec^2 on the sky, the entire chip thus covering a field of $2.'3 \times 3.'4$ of the sky. At the 234 cm telescope an Astromed GEC P8603 CCD detector with the format 385 $\times$ 578 pixels was used, a pixel here corresponding to 0.65 arcsec^2 on the sky, and the full CCD frame covering an area of approximately $4.' \times 6.'$ of it. Both CCD chips are blue coated. The read-out noise and electrons per ADU are respectively 1.4 and 14 for the Thomson CCD detector and 8 and 4 for the Astromed CCD detector. Bias and dark frames were taken intermittently. Flat field exposures were made on the twilight sky in each filter with exposure times ranging from 1 to 10 s. We have imaged five overlapping regions of the cluster at the 102 cm telescope and only one at the

Table 1. a) Details of cluster observations. Observations with 120-cm reflector

Filter	Region(s)	Exposure time (Sec)	Date
B	1	1800	3 March 89
V	1	900,120	3 March 89
I	1	300, 900	3 March 89
B	2	1800	4 April 89
V	2	900	"
I	2	360,60	"
B	1	900	30 January 90
V	1.2	900	"
I	1,2,3	360	"
B	2	1500	"
B	3	1500	31 January 90
V	3	900,300	"
B	3,4	1500	22 February 90
V	3,4	900	"
I	3,4	360	"
B	1,2	1200	4 March 92
V	1,2	900	"
I	1,2	300,120	"
I	4	360	"
B	5	1500	5 March 92
V	5	900	"
I	5	360	"

Table 1. b) Details of cluster observations. Observations with 234-cm Vainu Bappu Telescope

Filter	Exposure time (Sec)	No. of frames	Date
B	60	3	17 February 1994
	300	3	"
	900	1	"
	1200	2	"
V	15	4	"
	60	4	"
	300	4	"
	900	4	"

Table 2. Interval photometric errors as a function of brightness. σ is the standard deviation per observation in magnitude

Magnitude range	σ_B	σ_v	σ_I
$\leq$ 12	0.006	0.009	0.012
12.0 - 14.0	0.010	0.014	0.019
14.0 - 15.0	0.025	0.021	0.043
15.0 - 16.0	0.040	0.027	0.068
16.0 - 17.0	0.050	0.046	0.078
17.0 - 18.0	0.065	0.072	0.127
18.0 - 19.0	0.096	0.132	0.164
19.0 - 20.0	0.153	0.194	0.21

Table 3. Relative positions and CCD *BVI* magnitudes of stars measured in the field of NGC 2453. Stars observed by Gathier (1984), Moffat & Fitgerald (1974) and Seggewiss (1971) have been prefixed with G, MF and S respectively in the last column

Star	X (pixel)	Y (pixel)	V (mag)	(B-V) (mag)	(V-I) (mag)	Remarks
1	0.93	1092.16	17.87	0.67	0.84	
2	3.72	1233.55	18.69		1.34	
3	6.29	1227.45	17.44		1.07	
4	13.98	1170.03	16.83	0.58	0.71	
5	14.81	962.12	18.30		2.37	
6	19.14	833.04	19.02	0.61	1.18	
7	19.34	975.04	15.62	0.34	0.39	
8	26.14	1039.71	19.43		1.31	
9	33.07	984.41	17.97	0.90	0.89	
10	33.20	926.37	18.68	0.96	1.36	
11	33.22	784.26	14.53	0.34	0.47	MF33
12	35.57	1125.55	18.21	0.99	1.09	
13	37.06	833.89	18.42		2.53	
14	41.23	1133.77	15.67	0.41	0.55	
15	42.21	1116.93	17.64	0.70	1.04	
16	48.22	1171.72	18.61	0.91	1.41	
17	48.78	793.87	14.25	0.52	0.71	MF34
18	50.00	562.19	15.78	0.63	0.63	
19	55.09	854.50	17.88	0.74	1.03	
20	55.54	808.76	15.43	0.66	0.80	MF35
21	56.26	1171.29	18.65	0.99	1.18	
22	56.45	1012.27	14.04	0.21	0.25	MF1
23	64.22	1190.47	18.81		1.37	
24	68.05	350.09	16.20		0.77	
25	82.36	762.25	15.27	0.42	0.52	MF32
26	88.93	1207.14	16.78	2.03	2.30	
27	91.40	447.75	13.07	0.46	0.33	MF75
28	93.00	674.58	14.41	0.40	0.51	MF30,G430
29	93.15	810.52	16.81	0.79	0.92	
30	98.10	1111.39	18.08	0.90	1.07	
31	108.58	803.73	18.42	0.79	1.12	
32	117.01	418.13	19.01		1.68	
33	123.36	668.08	17.77	1.23	1.55	
34	127.76	1173.61	13.81	1.31	1.37	MF2
35	129.14	709.23	18.41	1.00	1.06	
36	130.57	743.60	14.59	0.42	0.45	MF31
37	133.93	1013.04	18.48	0.76	1.09	
38	138.57	715.11	18.60	0.96	1.13	
39	141.79	1071.22	16.94	0.49	0.61	
40	144.27	318.15	17.60		1.14	
41	145.51	754.76	17.24	0.68	0.76	
42	148.64	1106.13	18.79	0.78	1.21	
43	152.80	986.45	19.15		1.23	
44	154.23	795.53	17.66	0.73	0.91	
45	155.30	838.31	14.83	0.38	0.44	MF36
46	156.40	591.84	17.61		0.89	
47	159.27	932.92	15.08	0.40	0.49	MF42
48	159.56	681.26	15.02	1.18	1.28	MF29
49	160.17	644.57	17.46	0.78	0.79	
50	164.88	1059.27	17.69	0.84	1.01	
51	166.38	1242.63	17.80		1.07	
52	169.73	946.47	15.05	0.31	0.40	MF43
53	170.68	1087.23	16.56	0.38	0.56	
54	172.88	841.04	15.65	0.76	0.86	
55	175.40	1234.10	14.03	0.55	0.72	MF6
56	180.48	1083.88	14.69	1.13	1.32	MF4
57	182.06	578.09	12.55		0.43	MF28,G78
58	184.76	976.38	18.91		1.25	
59	187.19	797.93	18.55	1.13	1.00	
60	187.93	1125.26	15.41	0.32	0.41	MF3
61	190.42	758.17	18.34	1.49	1.85	
62	195.73	905.68	17.00	0.61	0.47	
63	196.53	1048.48	16.76	0.68	0.93	
64	198.65	912.09	15.30	0.49	0.60	MF41
65	198.68	851.16	15.58	0.57	0.72	MF37
66	198.89	744.51	18.22	0.87	1.01	
67	200.30	777.39	16.78	0.78	0.90	
68	203.95	850.22	16.54	0.61	0.58	
69	208.72	1124.42	18.44	0.80	1.12	
70	211.57	555.56	17.01	1.21	1.36	
71	212.94	1106.20	18.98	0.71	1.24	
72	213.03	1183.94	14.19	0.48	0.49	MF5
73	213.87	848.97	17.37	0.64	0.73	
74	216.98	896.93	12.85	0.43	0.23	MF40,G80
75	217.36	1137.83	19.24		1.27	
76	217.50	948.42	13.78	0.33	0.38	MF44
77	220.26	730.91	17.80	1.04	1.17	
78	220.65	1034.53	18.01	0.69	1.01	
79	224.20	926.67	18.38	0.77	0.75	
80	224.22	889.95	15.80	0.42	0.55	
81	227.37	514.06	19.21		1.34	
82	231.74	1222.91	18.96		1.52	
83	235.18	1231.58	17.83		0.98	
84	237.29	989.01	16.87	0.53	0.63	
85	243.43	868.35	13.09	0.25	0.26	MF38
86	244.50	824.73	18.00	1.03	1.27	
87	247.86	1120.81	17.77	0.82	0.97	
88	249.95	937.75	16.59	0.66	0.85	
89	250.37	361.89	18.88		1.60	
90	255.21	377.24	18.16		1.42	
91	257.34	1069.82	18.18	0.93	1.16	
92	260.45	885.41	14.59	0.30	0.42	
93	263.24	715.67	18.71	1.11	1.13	
94	265.04	450.08	16.53	0.87	0.82	
95	265.37	1037.01	16.26	0.43	0.51	
96	265.58	757.90	18.16	0.93	1.06	
97	266.22	809.03	16.10	0.41	0.44	
98	270.68	1238.07	16.91	0.12	0.68	
99	271.73	1216.74	18.61	1.13	1.32	
100	274.89	523.58	13.24	0.80	0.61	MF27
101	278.81	1028.66	17.08	0.94	1.07	
102	282.52	849.14	15.52	0.34	0.35	MF65
103	284.61	811.20	16.44	0.60	0.72	
104	285.27	488.48	16.63	1.16	0.97	
105	288.93	853.08	18.54		1.00	
106	289.42	893.13	19.18		1.34	
107	290.41	1142.47	19.17		1.26	
108	292.39	1121.10	18.83		2.28	
109	292.51	681.16	16.81	0.82	0.97	
110	293.20	576.21	16.26	0.94	0.84	
111	294.93	950.65	12.62	0.32	0.40	MF45,G82
112	295.02	1038.63	13.05	0.31	0.37	MF8,G69
113	300.57	846.27	14.10	0.43	0.46	MF64
114	300.96	718.93	17.57	0.78	0.94	
115	304.62	291.78	18.30		1.28	
116	305.01	1110.85	15.97	0.36	0.51	
117	307.86	1071.11	18.51	0.84	0.89	
118	309.05	1174.03	17.90	0.83	1.00	
119	309.07	321.20	17.00		1.07	

Table 3. continued

Star	X (pixel)	Y (pixel)	V (mag)	(B-V) (mag)	(V-I) (mag)	Remarks
120	312.42	1058.33	18.25	0.71	1.06	
121	315.56	794.55	16.67	0.59	0.71	
122	317.49	913.65	14.38	0.45	0.56	MF66
123	319.10	369.64	17.69		1.27	
124	326.62	756.83	16.60	0.53	0.50	
125	328.09	950.99	18.50		0.86	
126	330.41	1157.93	12.92	0.28	0.28	MF7,G68,S4
127	331.95	979.12	16.44	0.44	0.63	
128	333.18	355.54	19.16		1.60	
129	337.27	983.88	15.36	0.35	0.49	MF46
130	339.85	1073.10	16.07	0.60	0.74	
131	340.74	818.40	13.97	0.34	0.36	MF57
132	341.47	879.60	12.48	0.28	0.29	MF63,G93
133	343.19	847.15	16.21	0.42	0.48	
134	343.38	303.60	17.88		1.22	
135	344.71	942.98	18.29	0.79	1.09	
136	345.98	557.94	17.04	0.59	0.81	
137	347.11	786.31	13.80	0.35	0.45	
138	347.55	176.46	13.83	0.82	0.74	
139	348.11	824.76	16.62	0.44	0.54	
140	349.91	671.05	16.39	0.51	0.64	
141	350.18	909.33	14.96	0.38	0.47	MF62
142	350.44	848.10	17.00	0.58	0.71	
143	352.79	750.72	16.95	1.34	1.94	
144	352.81	532.79	15.75	0.82	0.78	
145	355.75	838.43	17.31	0.83	0.78	
146	356.35	916.39	13.12	0.28	0.33	MF61
147	359.09	809.67	14.47	0.35	0.36	MF56
148	359.34	881.77	16.80	0.54	0.44	
149	360.46	957.52	17.35	1.12	1.30	
150	362.93	909.79	17.33	0.56	0.81	
151	365.67	694.08	17.47	0.89	1.12	
152	368.07	806.83	15.08	0.63	0.70	
153	369.35	958.21	16.94	0.71	0.85	
154	371.20	1100.92	18.75		2.28	
155	371.46	896.74	13.81	0.29	0.35	MF60
156	371.66	722.07	16.33	0.53	0.62	
157	372.87	438.79	15.81		0.66	
158	373.21	1116.24	18.56	0.87	1.30	
159	375.47	841.79	12.73	0.28	0.28	MF58,G88
160	376.32	238.19	14.11	0.65	0.54	MF77
161	376.39	729.35	15.72	0.40	0.43	MF26
162	376.93	415.17	16.88	1.05	1.05	
163	376.97	534.55	16.90	1.07	1.05	
164	382.64	895.33	14.08	0.26	0.37	MF59
165	384.72	895.47	17.68		1.26	
166	384.90	851.47	18.08		1.11	
167	387.58	152.43	15.47	0.76	0.65	
168	387.91	1125.01	19.14		1.30	
169	388.61	1002.74	17.30	1.00	1.13	
170	391.61	534.79	18.09		1.34	
171	392.41	1234.07	19.48		1.38	
172	392.82	1035.66	15.84	0.69	0.84	
173	395.48	977.56	18.21	0.78	1.10	
174	396.03	889.26	17.92	0.84	1.23	
175	396.32	66.63	12.39	1.28	1.09	
176	398.50	1012.02	18.33	0.93	1.20	
177	399.63	1067.97	17.27	0.95	0.99	
178	401.22	1277.20	18.82		1.11	
179	401.86	77.67	15.22		0.46	
180	401.97	7.30	14.98	0.59	0.72	
181	402.60	767.49	15.97	0.67	0.75	
182	404.99	714.29	18.42	0.85	1.25	
183	405.59	1024.43	14.63	0.39	0.51	MF47
184	406.05	689.64	17.40	0.80	0.85	
185	406.89	820.68	15.24	0.61	0.76	MF53
186	408.41	902.46	18.74	0.67	1.23	
187	412.61	1203.40	16.84	0.65	0.83	
188	414.12	516.46	15.97		0.76	
189	414.27	845.00	18.07	0.58	1.01	
190	415.04	833.74	14.10	0.35	0.40	MF52
191	415.61	785.73	17.33	0.70	0.84	
192	418.01	1165.94	17.03	0.72	0.93	
193	423.77	382.45	18.06		1.11	
194	425.73	768.04	15.95	0.84	0.99	
195	426.68	1078.46	16.14		0.54	
196	429.90	1081.21	14.18	0.43	0.61	MF9,S6
197	433.25	810.82	15.55	0.49	0.57	
198	435.80	907.29	16.45	0.68	0.59	
199	436.12	917.53	17.31	0.99	1.22	
200	439.73	1305.82	16.55		1.03	
201	444.87	1009.36	18.83	0.88	1.32	
202	449.67	631.23	17.68		0.83	
203	450.07	306.14	15.38		1.25	MF78
204	452.38	881.41	15.24	0.40	0.48	MF51
205	453.46	803.77	18.57	0.78	0.92	
206	458.12	863.31	16.62	0.55	0.66	
207	460.47	1276.82	19.59		1.38	
208	460.75	979.38	16.08	0.49	0.64	
209	464.06	194.01	18.69		1.02	
210	465.00	950.55	16.09	0.76	0.83	
211	468.13	504.60	13.68	0.57	0.53	MF24
212	468.73	788.61	18.46	0.89	1.39	
213	468.85	878.18	15.91	0.48	0.63	
214	470.60	18.76	17.50		1.26	
215	471.72	1247.44	16.86	0.53	0.60	
216	472.60	1004.89	15.25	0.55	0.70	MF48
217	473.43	562.95	16.32	1.38	1.66	
218	476.78	489.44	17.67		0.88	
219	478.96	1046.16	15.26	0.35	0.42	MF13
220	479.52	762.09	17.79	0.77	1.08	
221	481.37	1134.53	15.53	0.78	0.92	
222	481.40	998.67	18.76		1.24	
223	485.42	987.62	14.78	0.29	0.39	MF49
224	486.47	1047.13	17.64	0.68	0.79	
225	487.42	1062.86	13.78	0.24	0.35	MF12
226	491.10	1162.47	16.70	0.87	1.13	
227	493.45	759.02	15.43	0.43	0.54	MF20
228	493.46	722.67	18.49		1.14	
229	495.25	531.13	14.22	0.60	0.53	MF23
230	496.25	437.17	18.29		1.05	
231	497.10	967.48	18.42	0.97	1.12	
232	497.60	1172.14	16.02	0.67	0.80	
233	498.33	1194.56	18.26	0.76	1.09	
234	499.80	1026.88	14.01	0.37	0.42	MF15
235	501.73	621.37	18.89		2.33	
236	503.97	301.48	18.40		2.52	
237	504.54	1200.37	16.73	0.58	0.79	
238	504.67	691.20	15.46	0.46	0.55	MF22

Table 3. continued

Star	X (pixel)	Y (pixel)	V (mag)	(B-V) (mag)	(V-I) (mag)	Remarks
239	509.94	472.46	18.85		1.66	
240	511.36	1034.83	16.72	0.60	0.83	
241	515.75	1044.46	14.92	0.45	0.51	MF14
242	517.34	533.77	17.85		1.12	
243	517.37	1118.29	16.92	0.72	0.90	
244	521.60	740.70	18.06	0.98	0.98	
245	523.49	353.30	17.63		0.64	
246	523.60	1211.93	18.29	0.80	1.05	
247	526.28	219.65	16.35	0.22	0.83	
248	530.11	512.14	18.41		1.26	
249	530.37	291.25	18.55		0.62	
250	531.16	637.14	16.75		0.69	
251	532.53	764.17	17.79	1.03	1.10	
252	533.63	1218.06	18.73	0.99	1.24	
253	537.04	529.69	18.48		2.26	
254	537.19	452.98	18.37		1.20	
255	538.05	740.22	16.41	0.54	0.64	
256	538.38	120.33	17.74		1.14	
257	539.55	130.16	17.15		1.21	
258	540.48	1220.18	16.71	0.46	0.67	
259	547.21	840.33	15.88	0.68	0.88	
260	549.52	1140.01	18.68		1.04	
261	553.24	636.40	18.16		1.04	
262	555.98	815.18	16.80	0.54	0.70	
263	559.05	990.48	13.16	0.24	0.36	MF16A,S3
264	561.23	934.52	18.98	0.75	1.23	
265	563.09	318.29	17.18		1.47	
266	563.84	232.64	15.39	0.51	0.76	
267	564.08	992.51	13.58	0.41	0.46	MF16B
268	568.58	701.23	14.47	0.38	0.46	MF21
269	570.03	894.87	15.74	0.41	0.52	
270	571.03	731.54	19.02		1.16	
271	573.49	278.99	17.87		2.39	
272	574.33	1183.31	13.92	0.47	0.60	MF10,S5
273	575.54	758.40	18.75	0.89	1.14	
274	577.65	541.08	16.62		0.91	
275	580.96	856.11	18.59		2.19	
276	584.18	55.21	17.25		0.97	
277	589.74	276.72	17.91		1.35	
278	591.11	950.44	17.27	0.61	0.65	
279	594.43	587.95	16.01		1.13	
280	597.01	839.87	18.94	0.81	1.22	
281	601.08	548.44	18.02		2.11	
282	610.79	346.01	18.00		1.22	
283	619.45	790.28	18.48		1.22	
284	620.11	740.67	18.24		1.11	
285	628.98	519.56	19.29		1.45	
286	629.98	428.51	16.71		0.84	
287	641.97	675.45	17.56	0.78	0.95	
288	643.70	278.41	18.16		1.29	
289	644.50	740.29	19.04		1.13	
290	646.38	568.10	18.40		1.12	
291	647.11	193.07	16.67		1.33	
292	650.37	487.39	17.89		1.22	
293	659.31	491.27	19.78		1.94	
294	663.27	515.07	17.84		1.29	
295	663.33	605.86	16.84	0.95	1.00	
296	673.94	299.61	16.69	0.60	1.08	
297	674.92	311.03	17.72		1.07	
298	676.87	86.56	18.24		1.14	
299	683.63	72.78	18.35		1.91	
300	690.15	612.29	19.13		1.43	
301	693.91	431.78	15.82	1.50	1.50	
302	694.01	660.70	16.38	0.81	0.89	
303	694.93	71.27	17.43		0.94	
304	697.85	791.78	16.06	0.43	0.61	
305	698.30	540.25	19.11		0.95	
306	703.20	509.75	14.42	1.13	1.43	MF81
307	712.33	249.81	16.68		0.88	
308	713.27	563.10	17.81		1.22	
309	713.64	646.44	14.37		1.34	MF85
310	715.49	319.55	17.69		0.96	
311	716.35	468.39	17.57		0.99	
312	719.55	229.34	15.63	0.65	0.63	
313	721.93	236.93	18.23		0.39	
314	731.68	476.04	15.67	0.76	0.86	
315	735.47	462.42	19.30		1.18	
316	736.85	566.30	15.79	0.37	0.56	
317	746.27	395.14	16.78		0.73	
318	750.79	787.85	16.34	1.02	1.13	
319	751.14	687.77	17.44		0.91	
320	752.29	503.83	18.41		1.15	
321	753.61	223.36	18.53		1.67	
322	758.30	513.69	16.75	0.91	0.87	
323	761.38	637.90	19.01		1.32	
324	764.02	433.04	14.52		0.66	
325	770.04	422.33	16.47		2.20	
326	775.63	581.64	16.62		1.93	
327	777.43	791.49	17.88		1.04	
328	779.14	157.51	17.34		2.09	
329	787.39	461.08	18.52		1.24	
330	789.54	228.80	17.24		2.31	
331	815.32	618.55	19.50		1.11	
332	818.35	533.63	13.47	0.26	0.41	MF82
333	821.20	705.32	17.96		1.05	
334	823.11	527.88	18.10		1.45	
335	825.90	608.03	16.14	0.75	0.81	
336	830.51	374.39	15.78	0.82	0.82	
337	838.37	671.85	19.04		1.12	
338	840.23	270.83	16.91		1.42	
339	845.76	489.69	18.83		1.34	
340	846.50	158.41	16.77		0.92	
341	852.21	533.12	17.36		0.88	
342	859.29	623.31	13.53	0.50	0.55	MF84
343	865.90	479.01	18.77		1.17	
344	866.91	738.31	18.69		1.32	
345	874.36	583.42	15.11	0.68	0.81	MF83
346	874.74	683.24	17.55		1.91	
347	875.09	446.01	15.57	0.54	0.50	
348	876.95	666.29	17.32		1.51	
349	884.77	151.45	17.93		1.01	
350	886.23	562.10	19.28		0.98	
351	889.17	600.87	18.19		1.18	
352	894.69	477.85	18.50		1.20	
353	895.10	583.16	18.79		0.94	
354	910.25	499.07	19.21		1.60	
355	914.36	787.52	15.82	0.71	0.90	
356	916.71	461.72	19.08		1.21	

234 cm telescope. Because of the larger field of the CCD detector at the 234 cm telescope, this one field nearly coincides with the five fields put together as imaged at the smaller telescope. In Fig. 1 a POSS red print of the cluster is displayed with the regions observed by us approximately marked. The imaged regions cover the cluster core maximizing thereby the number of measurable cluster members and minimizing the proportion of the field stars to be included in the cluster CMD's. Landolt (1983) standards covering a range in brightness ($9.2 < V < 13.4$) and in colour ($0.01 < V - I < 1.4$) were observed for calibration purposes.

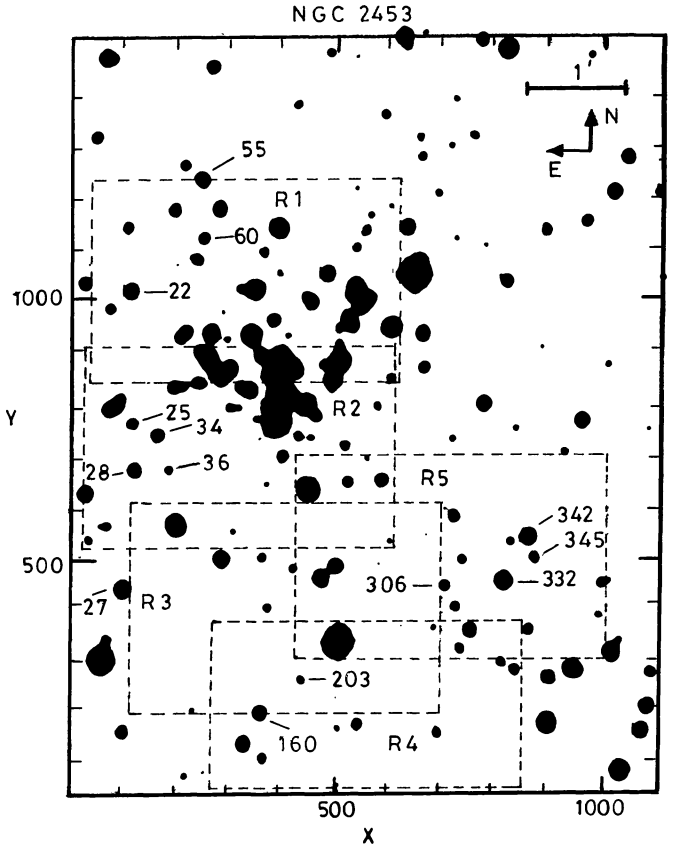

Fig. 1. Identification map for the imaged region of NGC 2453 as reproduced from the POSS blue print. The size of a CCD frame is 2.3 arcmin *times* 3.4 arcmin and the coordinates are in pixel units. A few stars from Table 3 are identified

1.2. *Data reduction*

The data were reduced at the Vainu Bappu Observatory using the Vax 11/780 computer and the COMTAL Vision image display station. The data frames were initially processed using the STARLINK package in the same way as described in Sagar & Pati (1989). Uniformity of the flat fields was found to be better than a few per cent in all the filters. Average flat fields were used in flat-fielding the CCD data frames.

The magnitude estimate of a star on a data frame has been obtained using the DAOPHOT software (Stetson 1987, 1992). The stellar point spread function used in the programme was evaluated from the sum of the uncontaminated images of several stars present on each frame.

The image parameters and errors provided by DAOPHOT were utilized in rejecting poor measurements. Only a few per cent stars got rejected in this process. The DAOMASTER software was used for cross identifying the stars measured on different frames in the cluster region. In those cases where the brighter stars are saturated on deep exposure frames, their magnitudes from the shorter exposure frames have been taken. This procedure limited us to stars fainter than $V = 12\overset{m}{.}0$ as stars with $V \leq 12\overset{m}{.}0$ were saturated on frames obtained even with the shortest exposure. Further processing and conversion of these raw instrumental magnitudes into the standard photometric system were done using the procedures outlined in Stetson (1992).

The colour equations for the CCD systems were determined by performing aperture photometry on the photoelectric standards. By fitting least square linear regressions to the observed aperture magnitudes as a function of the standard photometric indices, the following colour Eqs. (a) and (b) were derived respectively for the systems at 102 cm and 234 cm telescopes.

a)

$$\Delta b_{\rm CCD} = \Delta B + 0.05\ (\pm 0.02)\ (B - V),$$

$$\Delta \vartheta_{\rm CCD} = \Delta V - 0.03\ (\pm 0.005)\ (V - I),$$

$$\Delta i_{\rm CCD} = \Delta I + 0.04\ (\pm 0.005)\ (V - I).$$

b)

$$\Delta b_{\rm CCD} = \Delta B - 0.44\ (\pm 0.01)\ (B - V),$$

$$\Delta \vartheta_{\rm CCD} = \Delta V - 0.08\ (\pm 0.006)\ (B - V).$$

Here B, V and I are the standard magnitudes taken from Landolt (1983) and $b_{\rm CCD}$, $\vartheta_{\rm CCD}$ and $i_{\rm CCD}$ are the CCD aperture magnitudes.

To establish local standards we selected about twenty five isolated stars in the cluster region and used the DAOGROW programme to construct aperture growth curves required for determining the differences between the aperture magnitude and the profile fitting magnitude. These differences and differences in exposure times and atmospheric extinctions were used in evaluating the zero points for the reference cluster frames. The zero points are uncertain by 0.03 magnitude in B and by 0.02 magnitude in V and I. The internal errors estimated from the scatter in the individual measures of different exposures are listed

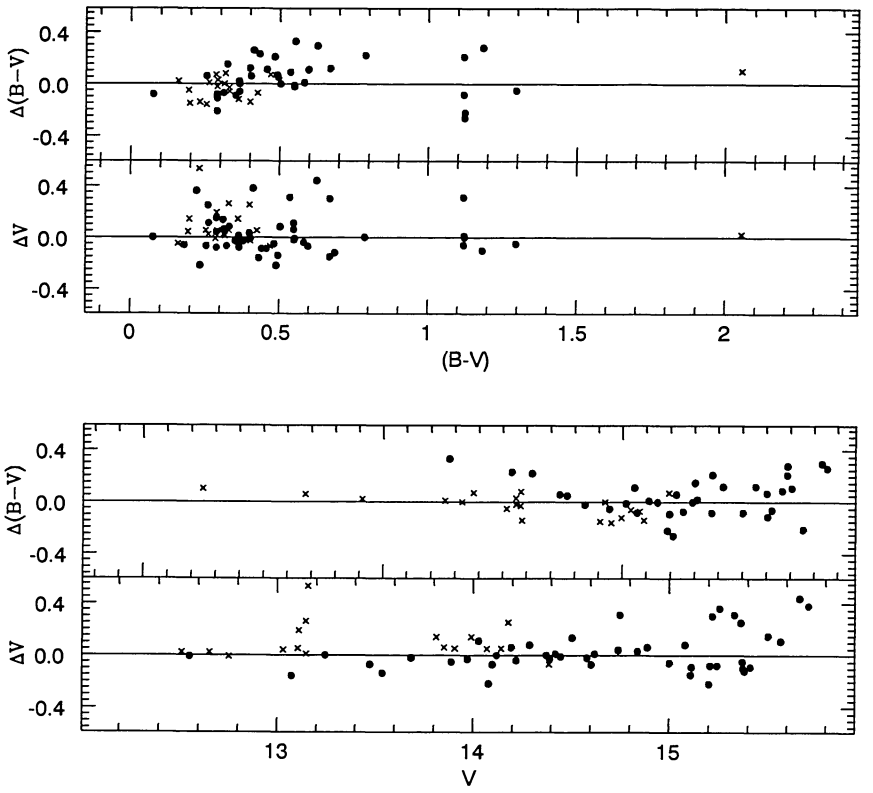

Fig. 2. A comparison of present photometry with data given by Moffat & Fitzzerald (1974). The differences (Δ) are in the sense present minus others' data, plotted against the CCD photometry. Photoelectric data are denoted by crosses while photographic data are denoted by filled circles

in Table 2 as a function of the magnitude for all the filters. The errors are larger ($\geq 0\overset{m}{.}10$) for stars fainter than $V = 17.0$. Table 3 lists all the stars thus processed with their x and y pixel coordinates (Cols. 2 and 3) as well as their V magnitudes (Col. 4) and the colours (Cols. 5 and 6). A handful of the bright stars are identified in Fig. 1. Stars common with Gathier, MF and Seggewiss have been identified in the last column by the letters G, MF and S respectively. We compare the present CCD photometry with the available photoelectric and photographic observations. The differences (denoted by "Δ") between the present data and the data obtained by others are plotted in Fig. 2 and the statistical results are listed in Table 4. These show that:

- i) The photoelectric data are in good agreement, in general, with the present CCD data. For a few stars discrepancies in $\mid \Delta V \mid$ are greater than $0\overset{m}{.}1$ An inspection of the CCD images indicates that the photoelectric measurements of the stars in question have been affected by the presence of a nearby star in each of these cases. The agreement between the photoelectric data and the present CCD data becomes excellent when the total light from the star and its companion in the CCD measurement is counted mimicking aperture photometry.

Table 4. Statistical results of the photometric comparison with Moffat & Fitzzerald (1974) data. The difference (Δ) is always in the sense present minus comparison data. The mean and standard deviation (σ) are based on N stars. A few points discrepant by more than 3.5 σ have been excluded from the analysis

	Δ V		Δ (B − V)	
Comparison data	Mean ± σ	N	Mean ± σ	N
Photoelectric	− 0.018 ± 0.044	13	0.013 ± 0.064	16
Photographic	+ 0.014 ± 0.076	34	0.05 ± 0.11	29

- ii) The photographic data show fair agreement ($\mid \Delta V \mid \leq 0\overset{m}{.}2$) with the present CCD data for stars brighter than $V \sim 15\overset{m}{.}0$. Near the limiting magnitude the photographic V magnitudes are systematically brighter than the CCD values (cf. Fig 2).
- iii) The scatter in the photographic data points is larger than the scatter in the photoelectric data points.

1.3. *Interstellar extinction*

Our data set did not allow a direct determination of the extinction to this cluster. We, therefore, depend upon the

results from the earlier photometric studies on the object (MF; Gathier 1984). We have adopted a value of $E(B-V)$ = 0.47 for the cluster. The data are insufficient to reveal any variation in reddening across the face of the cluster. Support for the adopted value of $E(B-V)$ comes from the general Galactic extinction pattern determined by Neckel & Klare (1980). According to the exinction-distance diagrams presented by these authors, the Galactic region of the cluster has a nearly constant A_v of 1^m to about 5 kpc and then an increase to $A_v \simeq 2$ at 6 kpc and beyond. Adopting a standard $R = 3.2$, a $E(B-V)$ of 0.47 gives A_v = 1.50 for the cluster which seems very reasonable. We shall return to this point in Sect. 4.

2. Results

2.1. *Radial distribution of stars in the cluster field*

We have studied the radial distribution of stars in the cluster field by dividing the entire field into concentric rings of 30 pixels each ($\sim$ 11 arcsec) with the centre at x_c = 360 and y_c = 880. The projected surface densities of all the stars and the stars brighter than 14^m in V have been plotted as a function of the angular radius in Fig. 3. The slopes obtained in a linear least-squares solution are respectively -0.649 ± 0.005 and -1.005 ± 0.008. Obviously the brighter stars are concentrated more in the central regions of the cluster. MF had determined the cluster radius to be about 2.4 and our data are in agreement with this value.

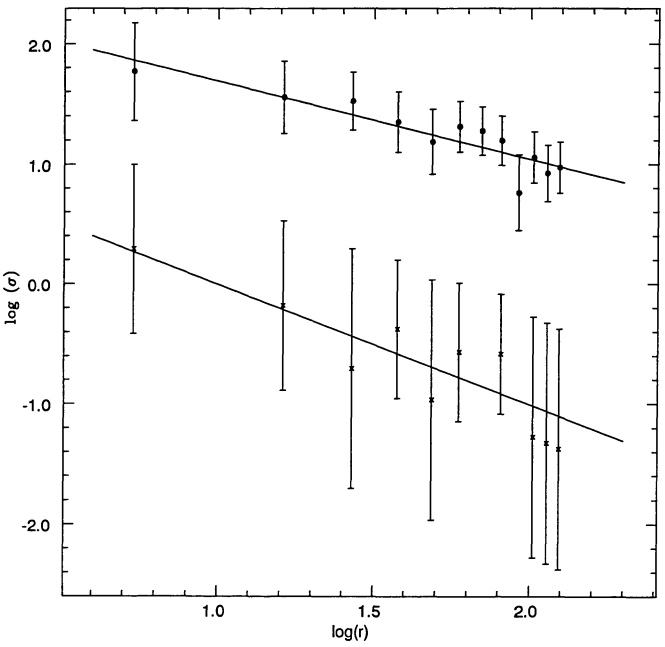

Fig. 3. Radial distribution of stars in the field of NGC 2453. Filled circles represent all stars while the crosses, offset by 1.0 in the y-axis, represent stars brighter than V=14 mag. Least square linear regression fits to the data points are superimposed

2.2. *Colour-magnitude diagrams and field star contamination*

The apparent colour-magnitude diagrams of NGC 2453 are displayed in Fig. 4. This includes all the stars we have observed. It is immediately obvious that the vast majority of the stars in the diagrams define a well populated cluster main sequence down to $V \sim$ 19.0. As anticipated some field star contamination is surely present, especially at the fainter end but the cluster sequence can be discerned without difficulty down to the faintest levels present in the data. Kinematic information on the cluster is extremely scanty and therefore, it is difficult to establish firmly the cluster membership of the stars seen in our images. In order to assess the the extent of field star contamination, we have divided the stars into two groups, 1 and 2, based on their projected distances from the cluster centre. Stars with coordinates - $x < 600$ pixels and $y > 600$ pixels (cf. Fig. 1) are placed in Group 1, while the remaining stars are placed in Group 2. The mean distance of the stars in Group 2 from the cluster centre is about 3 times as large as the mean distance from the cluster centre of the stars in Group 1. We may therefore consider stars in Group 2 as representative of the field star population. The area covered by stars in Group 2 is about 1.3 times the area covered by stars in Group 1. Frequency distribution of the stars of both the groups in different parts of the V, $V-I$ diagram normalised to the Group 1 area is listed in Table 5. We find that along the ZAMS, the number in Group 1 is generally more than the number in Group 2 and that the differences are statistically significant. The regions containing the field star samples (Group 2) are located about 3.5 arcmin away from the cluster centre while the cluster boundary/gravitational radius is only 2.4 arcmin (MF). This analysis indicates that contamination by field stars present in Group 1 may not affect the results of the present work.

This is the first time that the unevolved main sequence of the cluster has been observed. The main sequence is spread over four magnitudes in V. Width of the main sequence increases with faintness. This must be mainly due to observational errors. At fainter than $V \sim$ 15 magnitude it is difficult to separate field stars from the cluster members only on the basis of their closeness to the main populated area of the CM diagrams since at the distance of the cluster both field stars and cluster members occupy the same region of the CM diagrams. However, the probability of cluster membership should be small for the stars located well away from the cluster main sequence. The actual membership of the stars of the cluster can only be established through measurements of their proper motion and/or radial velocity. This remains to be done.

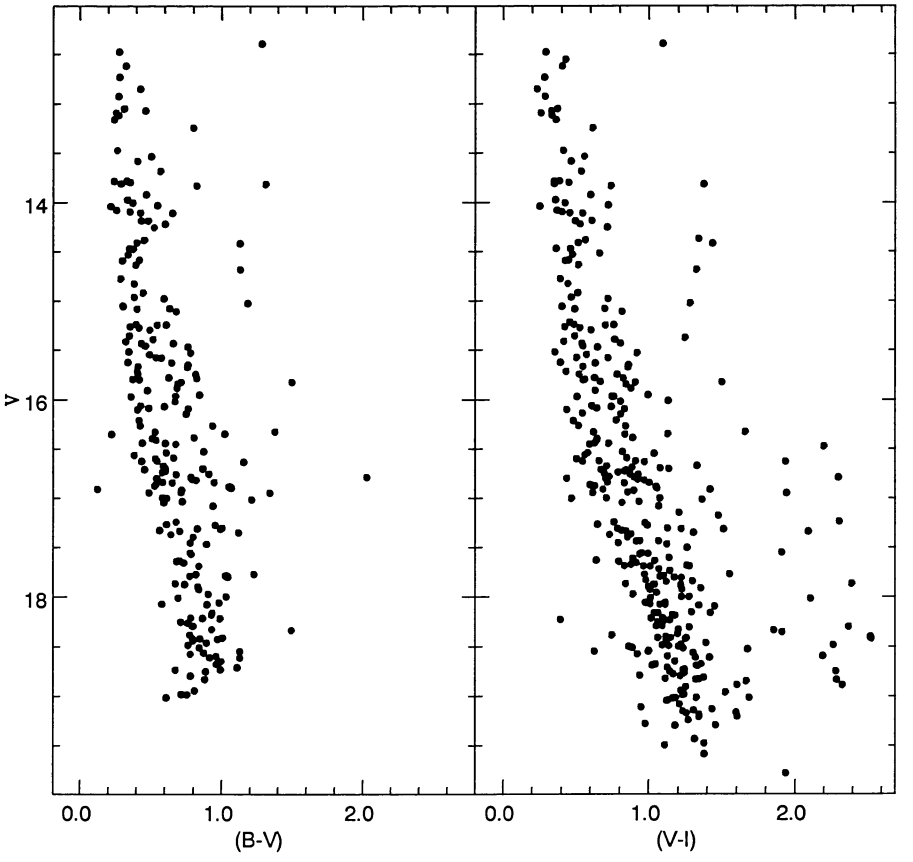

Fig. 4. The V, $(B-V)$ and V, $(V-I)$ apparent colour-magnitude diagrams for the NGC 2453

Table 5. Frequency distribution in the V, $V-I$ diagram of Group 1 and 2 stars. N_1 and N_2 denote the number of stars normalised to the same area in the Group 1 and 2 respectively. N_m denotes statistically expected number of cluster members

V	V − I								Total in all V − I		
	0.0 to 0.5		0.5 to 1.0		1.0 to 1.5		1.5 to 3.0				
	N_1	N_2	N_1	N_2	N_1	N_2	N_1	N_2	N_1	N_2	N_m
12 to 14	15	2	1	3	1	1	0	0	17	6	11
14 to 15	14	0	7	3	1	2	0	0	22	5	17
15 to 16	9	1	21	10	1	2	0	0	31	13	18
16 to 17	3	0	37	11	2	6	2	2	44	19	25
17 to 18	1	0	19	8	16	15	1	4	37	27	10
18 to 19	0	1	7	2	44	16	8	5	59	24	35

2.3. *Distance to the cluster*

In order to determine the distance modulus of NGC 2453, we have plotted in Figs. 5a and b the intrinsic V_0 vs. $(B-V)_0$ and V_0 vs. $(V-I)_0$ respectively of all the stars belonging to Group 1. In plotting this figure the apparent V, $B-V$ and $V-I$ magnitudes have all been corrected for interstellar reddening and extinction. We have used $E(B-V) = 0\overset{m}{.}47$ and the following relations from Walker (1987):

$$A_v = [3.06 + 0.25(B-V)_0 + 0.05E(B-V)] * E(B-V)$$

and $E(V-I) = 1.25 * E(B-V) * [1 + 0.06(B-V)_0 + 0.014\ E(B-V)]$.

The fiducial zero-age main sequence (ZAMS) from Walker (1985) was fitted in the V_0, $(B-V)_0$ and V_0, $(V-I)_0$ diagrams. After accounting for the dispersion in the colour expected from the error in the observations, the visual fits of the ZAMS to the bluest envelope of the CM diagrams leads to $V_0 - M_v = 13\overset{m}{.}80$ and $13^m.90$ respectively as indicated on the figure itself. Mean value of the true distance modulus is $13\overset{m}{.}85 \pm 0\overset{m}{.}2$ for NGC 2453. The uncertainty is estimated from the errors in observations, in the values of R and $E(B-V)$ and from the error in fitting the ZAMS. In Table 6 we present a comparison of our results with the ones obtained by other authors. Our value of the distance is closer to Gathier's. The accuracy of our result is much greater as we have been able to identify unambiguously the unevolved main sequence of the cluster

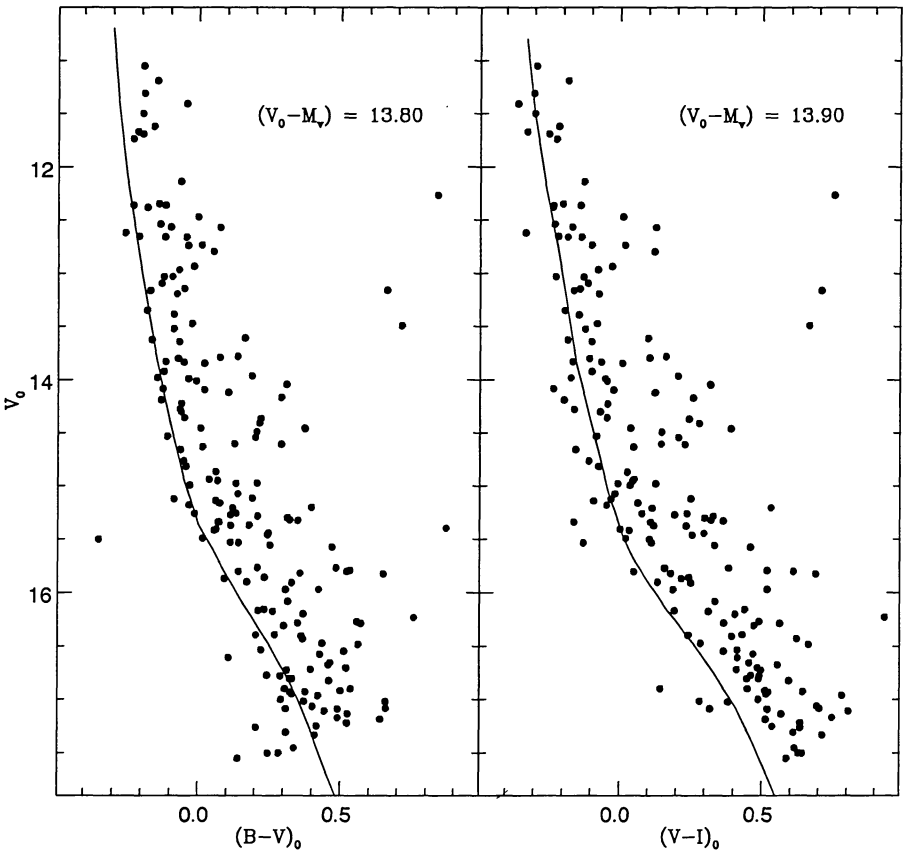

Fig. 5. The V_0, $(B-V)_0$ and V_0, $(V-I)_0$ diagrams for the Group 1 stars in the field of NGC 2453. Continuous curves are the ZAMS fitted to the unevolved part of the cluster MS for the values indicated in the diagram. The true distance modulus to the cluster is 13.9 mag

unlike in MF where only an evolved cluster sequence was observed.

Table 6.

Reference	Faintest V mag observed	E (B−V)	D (kpc)	Method
MF	15.5	0.47 ± 0.04	2.9 ± 0.3	Main Sequence fitting
Gathier	14.4	0.49 ± 0.01	5.0 ± 0.6	Photometric method
This work	20.0	0.47	5.9 ± 0.5	ZAMS fitted over a wide range in V
Seggewiss	13.93	0.48	1.50	ZAMS fitting

2.4. *Age of the cluster*

Figure 6 displays a plot of the absolute magnitude M_v against $(B-V)_0$ of all the stars in Group 1 in the field of NGC 2453. A uniform colour excess $E(B-V) = 0^m.47$ has been applied to all of them and a true distance modulus of $13^m.85$ has been used. Photometric data for members brighter than $V = 12$ (i.e. $M_v = -3^m.30$) have been taken from MF as their brightness precluded any possibility of our deriving reliable parameters for them using, as we have done, the techniques of faint star photometry. There are three such members. We have estimated the age of the cluster by fitting stellar evolutionary isochrones given by Schaller et al. (1992) to the M_v, $(B-V)_0$ diagram. The isochrones have been computed for Population I stars ($X = 0.68$, $Y = 0.30$, $Z = 0.02$) and the evolutionary models include the effects of mass loss and convective core overshooting. From a close scrutiny of the diagram we infer that stars brigter than $M_v = -2.0$ show evolutionary effects. As present observations cannot decide the status of their cluster membership, an accurate determination of the age of the cluster is not possible. The isochrones fitting the bright end of the MS, the blue giant MF 54 and the red giant MF 50 indicate an age between 15 and 40 Myr with a mean age of about 25 Myr. The turn-off point is located approximately at $M_v = -1^m.5$ and $(B-V)_0 = -0^m.22$. This is consistent with the age estimate given as is seen from the calibration of the colour at turn-off versus the age given by Maeder & Meynet (1991).

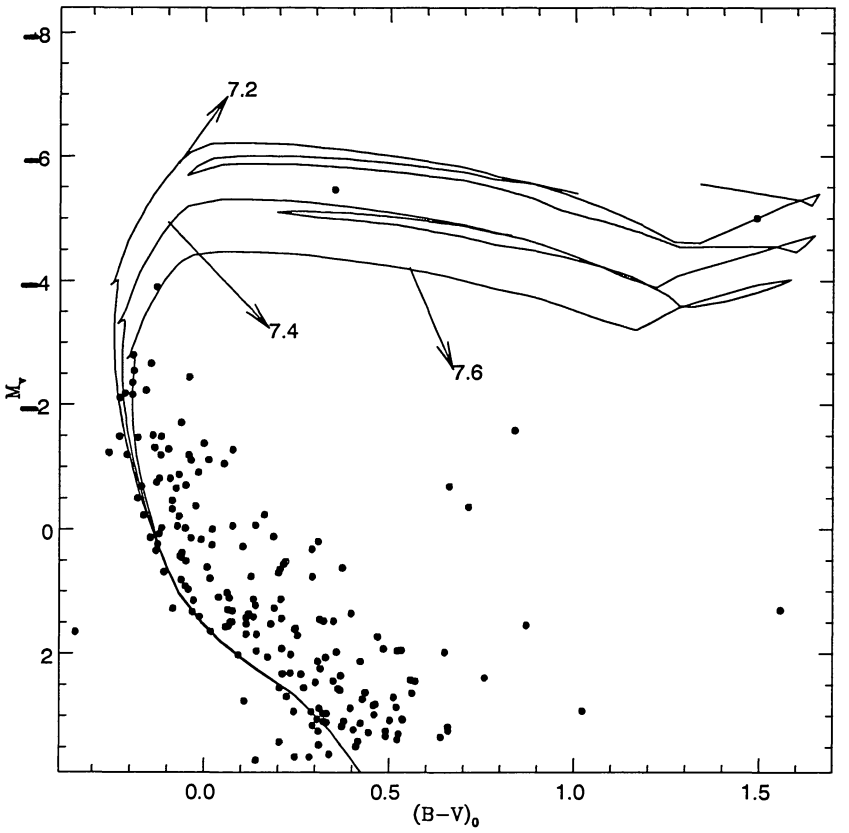

Fig. 6. The M_0, $(B-V)_0$ diagram for the Group 1 stars in the field of NGC 2453. Isochrones from Schaller et al. (1992) for Pop I stars have been fitted to the bright cluster members. They indicate that the age of the cluster is between 15 to 35 Myrs

Our inferred age agrees fairly well with MF who used older isochrones due to Wilde (1968).

3. Discussions and conclusions

Deep BVI CCD photometry of NGC 2453 indicates that the open cluster is young (age $\leq$ 40 Myr) and lies at a distance of nearly 6 kpc from us. Velocity data of stars in the field are extremely scanty, the only measurement available being the radial velocity of the star MF 54, a blue giant. The cluster perhaps contains a bright red giant, MF 50, of spectral class K3 -5 II/Ib. Lapasset et al. (1991) observed this star in the UBV-DDO system and found it to be variable. The mean distance modulus of the cluster is $13\overset{m}{.}85 \pm 0\overset{m}{.}20$ corresponding to a distance of 5900 $\pm$ 250 pc. The upper main sequence of the cluster shows signs of evolution and the use of this in fitting the ZAMS led to the wrong estimate of the distance in MF. Our CCD frames have gone much deeper uncovering for the first time the unevolved main sequence of the cluster. We have shown by use of statistical criteria that the majority of the stars belong to the cluster sequence. Further the radial distribution of stars in the CCD frames shows that the bright stars are concentrated more towards the centre of the cluster. The scatter in the colour-magnitude arrays does increase at the fainter end due to field star contamination. However, the main sequence is clearly discernible to these limits and it is highly unlikely that the presence of a small fraction of field stars in the colour-magnitude diagrams will affect the distance determination in any significant way. There are no published results on the expected field star distribution in number and colour at the position of the cluster or in its vicinity. Hence a model estimate of the field star contamination was not possible. The age determination is not so certain as the membership of stars MF 50 and 54 has not been clearly established. Isochrone fitting indicates an age in the vicinity of 15–40 Myr with a mean age of about 25 Myr.

At a distance of 6 kpc in the third quadrant of the Galaxy (l = 243°.3) the expected radial velocity of the cluster due to circular motion around the centre is 70 km s^{-1}. The measured radial velocity of 67 km s^{-1} for the star MF 54 is thus consistent with this star being at 6 kpc. The relative youth of this star ensures that its deviation from circular motion is small. Since the expected cluster radial velocity and the radial velocity of this particular star are close to each other, it lends some support to the premise that MF54 is a cluster member. Gathier (1984) had excluded this star from the determination of the distance to the cluster since its low gravity posed problems

for an accurate determination of its M_v. Until proper motion and radial velocity data are available for the cluster the membership question will remain open. The cluster lies in a direction of low interstellar extinction. This is evident from the maps of the region as reproduced in Neckel & Klare (1980). For the lack of measurements in U we could not determine the reddening to the cluster independently. It does appear, however, that the cluster lies in a region of normal interstellar reddening. We have tried to fit the ZAMS to V, $B-V$ and V, $V-I$ diagrams keeping the distance modulus the same while varying independently $E(B-V)$ and $E(V-I)$. The values $E(B-V) = 0.47$ mag and $E(V-I) = 0.58$ mag are seen to produce reasonably good fits. The ratio $E(V-I)/E(B-V) = 1.23$ then indicates that the reddening is normal.

We embarked on this study of the cluster NGC 2453 with the hope that we would be able to establish a physical association of the planetary nebula NGC 2452 with it. Had we succeeded, exciting possibilities would have opened up of studying in detail stellar evolutionary aspects of PN progenitors in clusters. The distance to NGC 2452 has been measured by a number of authors using a variety of methods including statistical ones. The reddening- distance method leads to the largest value of it namely 3.57 ± 0.47 kpc. All other methods yield shorter distances. Therefore, our results indicate that the physical association of the nebula with the cluster is highly unlikely. Our analysis puts the cluster far beyond the nebula at a distance of 5.9 ± 0.2 kpc. We have revised upward the distance obtained by Gathier (1984) by a factor of about 1.2. The PN is most likely a foreground object. In the reddening - distance diagram for NGC 2452 as obtained by Gathier (1984) the crucial data point was the one pertaining to NGC 2453 and this was given a weightage of ten. Although our determination of the distance to NGC 2453 is yet more accurate, the increase of 18% is not large enough to make a substantial difference to the reddening - distance relation depicted in Gathier's work. Therefore the distance to NGC 2452 estimated by this method will not be altered beyond the errors quoted in Gathier. Since the Galactic region 89 (242/0.0) where NGC 2452 & 2453 are located, is one of constant A_v of about $1^m.0$ up to 5 kpc or a little beyond, it is not surprising that the $E(B-V)$'s of the cluster and the foreground nebula are so similar. The coincidence in radial velocities mentioned in the introduction need not weigh us down either. Planetary nebulae are known to show marked departures from circular motion. At the distance of the nebula from the Galactic Centre the circular motion produces a positive radial velocity of 39 km s^{-1}. The measured radial velocity of 68 km s^{-1} of the nebula shows a peculiar motion on the order of 30 km s^{-1} which is entirely reasonable even for a Type I planetary nebula. We conclude therefore that NGC 2452 and NGC 2453 are not physically associated at all and there is no compelling observational evidence to cast any further doubt on this inference.

Acknowledgements. We thank the referee Dr. S. Ortolani for constructive criticisms that helped us improve the paper.

References

Campbell W.W., Moore J.H., 1918, Publ. Lick Obs. 13, 75
Gathier R., 1984, Ph. D. thesis, Univ. Groningen
Landolt A.R., 1983, AJ 88, 439
Lapasset E., Claria J.J., Minniti D., 1991, IBVS No. 3544
Lyngå G., 1987, Catalogue of Open Cluster Data, CDS Strasbourg
Maeder A., Meynet G., 1991, A&AS 89, 451
Mallik D.C.V., Sagar R., Pati A.K., 1993, in IAU 155: Planetary Nebulae. In: Weinberger R. and Acker A. (eds.). Kluwer Academic Publishers, p. 182
Moffat A.F.J., Fitzgerald M.P., 1974, A&AS 18, 19 (MF)
Neckel Th., Klare G., 1980, A&AS 42, 251
Sagar R., Pati A.K., 1989, Bull. ASI 17, 6
Schaller G., Schaerer D., Meynet G., Maeder A., 1992, A&A 96, 269
Seggewiss W., 1971, Veröffentl. Astron. Inst. Bonn, Nr. 83, 21
Stetson P.B., 1987, PASP 99, 191
Stetson P.B., 1992, in Astronomical Data Analysis Software and Systems I. In: Worrall D.M., Biemesderfer C. and Barnes J. (eds.), ASP Conf. Ser. 25, p. 297
Walker A.R., 1985, MNRAS 213, 889
Walker A.R., 1987, MNRAS 229, 31
Wilde K., 1968, Dissertation, Univ. Sternw. Göttingen